DESY 08-076
HD-THEP-08-13
PITHA 08/12

DESY 08-076
HD-THEP-08-13
PITHA 08/12

Squarks and gluinos at a TeV e^+e^- collider:

Testing the identity of Yukawa and gauge couplings in SUSY-QCD

A. Brandenburg*
Deutsches Elektronen Synchrotron DESY, D-22603 Hamburg, Germany
M. Maniatis
Institut für Theoretische Physik, Philosophenweg 16, D-69120 Heidelberg, Germany
M.M. Weber
Department of Physics, University at Buffalo, Buffalo, NY14260-1500, USA
P.M. Zerwas
Inst. Theor. Phys. E, RWTH Aachen U., D-52074 Aachen, Germany and
Deutsches Elektronen Synchrotron DESY, D-22603 Hamburg, Germany

arXiv:0806.3875v1 [hep-ph] 24 Jun 2008

Supersymmetry predicts the identity of Yukawa and gauge couplings in the QCD sector: $q\tilde{q}\tilde{g} = \tilde{q}\tilde{q}g = qqg$. We examine whether the $q\tilde{q}\tilde{g}$ Yukawa coupling can be determined, by methods complementary to LHC, by analyzing squark-gluino final states at a TeV e^+e^- collider.

1. Introduction

While in QCD non-Abelian gauge invariance leads to equal couplings for quarks and squarks to gluons, supersymmetry guarantees the identity of the Yukawa coupling between squarks, quarks and gluinos with the gauge coupling, cf. [1, 2, 3]:

$$\hat{g}_s(q\tilde{q}\tilde{g}) = g_s(\tilde{q}\tilde{q}g) = g_s(qqg)\,. \tag{1}$$

This identity is preserved if supersymmetry is broken by soft terms, *i.e.* gaugino/scalar masses, and bi/tri-linear couplings between scalar fields. The relation is crucial for the natural extension of the theory from the electroweak scale to the Planck-scale without introducing quadratic divergences, which are generated in the squark propagator, for instance, by the bosonic squark/gluon loops and which are canceled by the fermionic quark/gluino loop.

Several methods can be exploited to test the identity (1) by measuring the magnitude of the Yukawa coupling $q\tilde{q}\tilde{g}$. At the LHC the production of squark pairs in quark-quark collisions which is mediated solely by the interchange of gluinos, provides a classical instrument for the measurement of the Yukawa coupling in SUSY-QCD [4]. In practice, however, an ensemble of auxiliary measurements of decay branching ratios is necessary, presumably requiring LC supplements, if the coupling should be determined in an [almost] model-independent way.

A potential complement to this method is gluino emission in association with quark-squark final states in e^+e^- collisions, *cf.* Refs. [5, 6]:

$$e^+e^- \to q\tilde{q}\tilde{g} \tag{2}$$

* *Present address:* Genedata AG, CH-4016 Basel, Switzerland

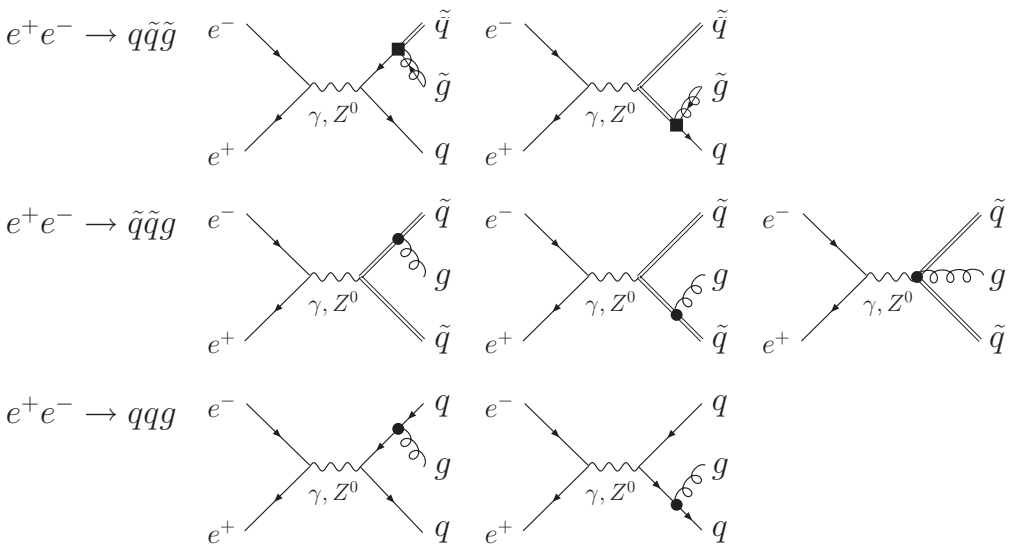

Figure 1: *Generic Born diagrams corresponding to the processes (2) and (3),(4) which are proportional to the Yukawa coupling $\hat{g}_s$ [box] and to the gauge coupling g_s [dot], respectively.*

which requires a non-zero Yukawa coupling. This process is related by supersymmetry directly to the gauge processes of gluon radiation off squarks,

$$e^+e^- \to \tilde{q}\tilde{q}g\,, \tag{3}$$

and standard gluon radiation off quarks,

$$e^+e^- \to qqg\,. \tag{4}$$

Generic diagrams are displayed in Fig. 1. [Note that the abbreviations $qq..$, used for notational clarity, should anywhere be interpreted as the incoherent sum of particle-antiparticle plus antiparticle-particle states of all flavors and L, R indices.] It can be anticipated without analyzing details that the process (2) will be useful in practice only if the squarks and gluinos are moderately light; the range, however, is quite compatible with electroweak precision analyses, cf. Ref. [7]. The process is suppressed by the [small] Yukawa coupling squared, the propagator transporting high (virtual) masses, and the 3-body phase-space involving two heavy particles; the suppression remains effective even significantly above the threshold.[1] Nonetheless, the production cross sections are in general expected still to be considerably larger than loop-mediated gluino-pair production in e^+e^- collisions [9].

Since any method for measuring the SUSY-QCD Yukawa coupling is connected with ancillary problems, it is worth studying to what extent the process (2) could be exploited to approach a solution of this experimental challenge. Since the identity of Yukawa and gauge couplings is a central concept of supersymmetric theories, it is mandatory to study all opportunities which could shed light on this aspect. To reach solid conclusions, the theoretical analysis has been performed including SUSY-QCD corrections at next-to-leading order [NLO] which increase the complexity of the theoretical work enormously. In turn, this allows us to study the sensitivity of SUSY-QCD corrections in $\tilde{q}\tilde{q}$, qq final states to the Yukawa coupling. Preliminary results had been contributed to conference proceedings [10].

[1] These difficulties contrast with measurements of the Yukawa couplings in the electroweak SU(2)×U(1) sector in which chargino, neutralino and selectron pair-production in polarized e^+e^- and e^-e^- processes allow the determination of the electron-related Yukawa couplings at the per-cent down to the per-mill level [8].

	Energy window	Final states with strong gauge / Yukawa couplings			
			α_s	$\hat{\alpha}_s$	$\hat{\alpha}_s^2$
	$2m_{\tilde{q}} \le \sqrt{s} \le m_{\tilde{q}} + m_{\tilde{g}}$	$\tilde{q}\tilde{q}(2j+\not{E})$	$\tilde{q}\tilde{q}g(3j+\not{E})$		
$m_{\tilde{q}} < m_{\tilde{g}}$	$m_{\tilde{q}} + m_{\tilde{g}} \le \sqrt{s} \le 2m_{\tilde{g}}$	$\tilde{q}\tilde{q}(2j+\not{E})$	$\tilde{q}\tilde{q}g(3j+\not{E})$	$q\tilde{q}\tilde{g}(4j+\not{E})$	
	$2m_{\tilde{g}} \le \sqrt{s}$	$\tilde{q}\tilde{q}(2j+\not{E})$	$\tilde{q}\tilde{q}g(3j+\not{E})$	$q\tilde{q}\tilde{g}(4j+\not{E})$	$qq\tilde{g}\tilde{g}(6j+\not{E})$
	$2m_{\tilde{g}} \le \sqrt{s} \le m_{\tilde{q}} + m_{\tilde{g}}$				$qq\tilde{g}\tilde{g}(6j+\not{E})$
$m_{\tilde{q}} > m_{\tilde{g}}$	$m_{\tilde{q}} + m_{\tilde{g}} \le \sqrt{s} \le 2m_{\tilde{q}}$			$q\tilde{q}\tilde{g}(6j+\not{E})$	$\langle qq\tilde{g}\tilde{g}(6j+\not{E})\rangle$
	$2m_{\tilde{q}} \le \sqrt{s}$	$\tilde{q}\tilde{q}(6j+\not{E})$	$\tilde{q}\tilde{q}g(7j+\not{E})$	$\langle q\tilde{q}\tilde{g}(6j+\not{E})\rangle$	$\langle qq\tilde{g}\tilde{g}(6j+\not{E})\rangle$

Table I: *Kinematically accessible processes involving squarks and gluinos at different c.m. energies for $m_{\tilde{q}} < m_{\tilde{g}}$ and $m_{\tilde{q}} > m_{\tilde{g}}$. Processes are identified by the jet topology of the final states. The corresponding gauge and Yukawa couplings are denoted by $\alpha_s = g_s^2/4\pi$ and $\hat{\alpha}_s = \hat{g}_s^2/4\pi$, respectively. [Final states in $\langle ... \rangle$ brackets in the second part of the table are generated primarily by squark decays to gluinos to which the power counting of the couplings does not apply.]*

2. Squarks and gluinos in e^+e^- collisions

Before discussing the dependence of individual processes on the SUSY-QCD Yukawa coupling, an overview should be given on the size of cross sections which can naturally be expected for experimental analyses. In addition, the key points of the crucial techniques used in the higher-order calculations are summarized. For the reader's convenience, we include some earlier material from the literature as to provide a coherent presentation of the problems.

The topology of the final states after the decays of the supersymmetric particles down to the LSP [assumed to be the lightest neutralino $\tilde{\chi}_1^0$ in the present R-parity conserving set-up] depends strongly on whether squarks are lighter or heavier than gluinos. In the first scenario, squarks decay preferentially to charginos/neutralinos, while gluinos decay to squark-quark pairs, followed by the subsequent squark decays,

$$\begin{aligned} m_{\tilde{q}} < m_{\tilde{g}}: \quad & \tilde{q} \to q + \tilde{\chi} \to j + \not{E}, \text{ etc} \\ & \tilde{g} \to \tilde{q} + q \to q + q + \tilde{\chi} \to jj + \not{E}, \text{ etc}\,. \end{aligned} \tag{5}$$

In the second scenario squarks decay to gluinos which subsequently decay, mediated by virtual squarks, to charginos/neutralinos,

$$\begin{aligned} m_{\tilde{q}} > m_{\tilde{g}}: \quad & \tilde{q} \to \tilde{g} + q \to \tilde{q}_{\rm virt} + q + q \to q + q + q + \tilde{\chi} \to jjj + \not{E}, \text{ etc} \\ & \tilde{g} \to \tilde{q}_{\rm virt} + q \to q + q + \tilde{\chi} \to jj + \not{E}, \text{ etc}\,. \end{aligned} \tag{6}$$

In contrast to QCD jets, the jets in heavy squark/gluino decays are well separated in phase space, and clustering will occur only at random. A large fraction of the charginos/neutralinos $\tilde{\chi}$ is in general light and, if not the LSP, they decay to leptons [with taus generating only slim jets with up to three hadrons which we keep separate in the jet counting.]

A survey of all squark and gluino production processes relevant for investigating the strong gauge and Yukawa couplings is given in Tab. I which indicates the threshold energies and the jet topologies for the individual continuum processes in which $\tilde{q}$ or $\tilde{g}$ are not mutual decay products [QCD coupling $\alpha_s = g_s^2/4\pi$; Yukawa coupling $\hat{\alpha}_s = \hat{g}_s^2/4\pi$]. At the time when the measurement of the Yukawa coupling can be performed, the masses of the supersymmetric particles will be determined very precisely, *cf.* Ref. [11], and it will be evident which part of the table is relevant.

It may be noted that final states of events generated by the decay of on-shell squarks to quarks and the lightest neutralino as LSP, $\tilde{q} \to q + \tilde{\chi}_1^0$, can be reconstructed up to a two-fold ambiguity, an important identification tool when the squark and neutralino masses are known, *c.f.* Ref. [12]. As the $\tilde{q}\tilde{q}$ c.m. frame [denoted by $*$]

coincides with the laboratory frame, or, can be reconstructed after gluon emission, the $\tilde{q}\tilde{q}$ axis in that frame is given by one of the two intersections of the cones centered at the quark axes with opening angles determined from $m^2_{\tilde{\chi}} = m^2_{\tilde{q}} - 2E^*_q E^*_{\tilde{q}}(1 - \beta^*_{\tilde{q}} \cos\theta^*_{\tilde{q}})$. The false solutions for the axes give rise to essentially flat background angular-correlations.

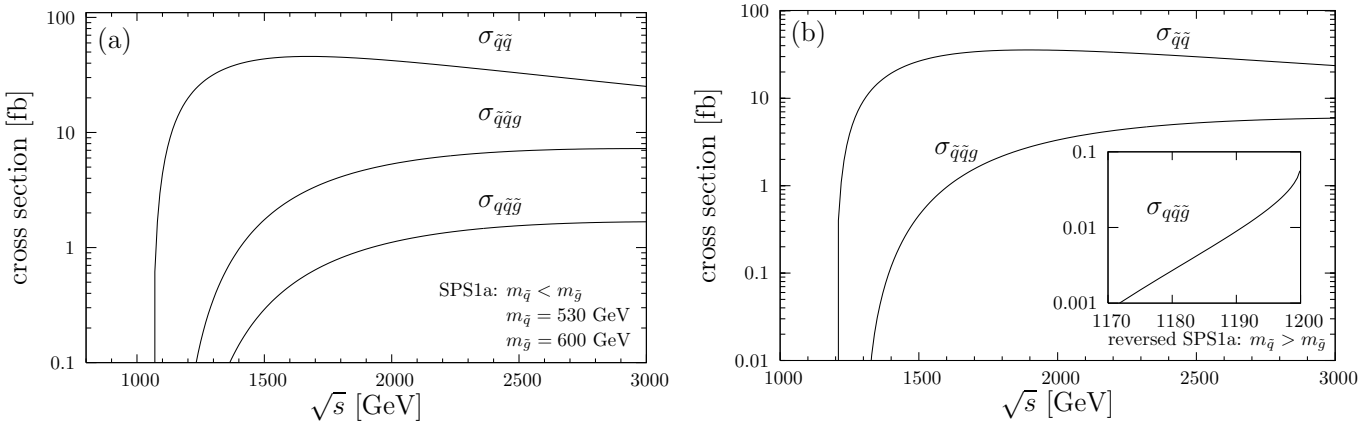

Figure 2: *Relevant tree level cross sections for the production of squarks and gluinos. In Fig.(a) the gluino is assumed to be heavier than the squarks, according to the SPS1a scenario, and in Fig.(b) the* reversed *mass scenario is considered, where the gluino is lighter ($m_{\tilde{g}} = 530$ GeV) than the squarks (degenerate squark masses $m_{\tilde{q}} = 600$ GeV).*

Leaving out rare processes of second order in the Yukawa coupling, the cross sections for squarks lighter than the gluino are displayed in Fig. 2(a), summed over five flavors. For clear identification a minimal energy cut $E_X > 100$ GeV is applied to the gluon jet (details are given in the following subsections). In Fig. 2(a) production cross sections are shown for squark and gluino masses adopted from the standard SPS1a scenario [13], i.e. $m_{\tilde{g}} = 600$ GeV and a common squark mass of $m_{\tilde{q}} = 530$ GeV, [which is compatible with the mass limits allowed by the searches for supersymmetric particles at the Tevatron [14]]. The dominant cross section of the $\tilde{q}\tilde{q}$ final state rises steeply above the threshold proportional to the third power of the velocity of the squarks. Since the gluino is heavier than all squarks in the SPS1a scenario, the production threshold for the $q\tilde{q}\tilde{g}$ final state is higher than the $\tilde{q}\tilde{q}$ threshold. The jet topologies in the final states are characteristic for the individual processes and jet counting can be used as a powerful discriminant. [Of course, this Born approach must be refined by properly controlling QCD showers in experimental analyses.]

The relevant cross sections for the scenario in which the squarks are heavier than the gluinos, are shown in Fig. 2(b). In a merely *ad hoc* procedure, as any details beyond SUSY-QCD are irrelevant for the present discussion, the mass values of squarks and gluino in SPS1a are just reversed. [Such a scenario is actually close to SPS4.] Note that above the c.m. energy of twice the squark mass the process $q\tilde{q}\tilde{g}$ proceeds primarily through squark pair production with subsequent decay of a squark into a gluino. The energy window for $q\tilde{q}\tilde{g}$ production *sui generis* is narrow and the cross section of the process, due to phase space suppression near the threshold, is rather small.

However, an additional opportunity for measuring the Yukawa coupling in the second scenario is provided by the squark decays to gluinos, Ref. [15]. The threshold behavior of the squark-excitation cross section in e^+e^- collisions depends sensitively on the total decay width $\Gamma(\tilde{q})_{tot}$. This method of measuring the total width was discussed in Ref. [8] for slepton production but it can be transferred to squarks in the same way; in fact, the impact of the total width on the production cross section for squarks is significantly bigger as a result of the increased size of the width. On the other hand, the electroweak continuum cross section for squark-pair production with squarks decaying to gluinos is proportional to the branching ratio $BR(\tilde{q} \to q\tilde{g})$ squared. By combining the two threshold and continuum

measurements of total width and branching ratio, respectively,

$$\Gamma(\tilde{q} \to q\tilde{g}) = BR(\tilde{q} \to q\tilde{g}) \times \Gamma(\tilde{q})_{tot} = \frac{\hat{g}_s^2}{6\pi} m_{\tilde{q}} \left(1 - \frac{m_{\tilde{g}}^2}{m_{\tilde{q}}^2}\right)^2 , \tag{7}$$

the SUSY-QCD Yukawa coupling can be determined from the partial width.

Since in the analysis of the individual channels higher-order SUSY-QCD corrections will be included, the technical set-up should be summarized globally. To take advantage of our extensive infra-structure, the dimensional regularization has been carried out in the DREG scheme. To comply with the SUSY-QCD Ward identities, which are violated by the mismatch of fermionic and bosonic degrees of freedom in this scheme, counter terms must be added which however can be mapped onto a modified relation between gauge and Yukawa couplings [15, 16]:

$$\hat{g}_s = g_s \left[1 + \frac{\alpha_s}{4\pi}\left(\frac{2}{3}C_A - \frac{1}{2}C_F\right)\right] = g_s \left[1 + \frac{\alpha_s}{3\pi}\right] . \tag{8}$$

The masses of the heavy particles, squarks and gluinos, are introduced as pole masses. For the renormalization of the couplings the $\overline{\rm MS}$ scheme is adopted. The "experimental" QCD gauge coupling $\alpha_s^{(5)}(Q^2)$ is introduced for five massless quarks and all heavy particles are decoupled. From this coupling, conventionally fixed at the energy $Q = M_Z$, Ref. [17], the appropriate QCD gauge coupling for the SUSY system, $\alpha_s(Q^2)$, above the heavy particle thresholds can be derived as

$$\alpha_s(Q^2) = \alpha_s^{(5)}(Q^2)\left[1 + \frac{\alpha_s^{(5)}(Q^2)}{2\pi}\left(\frac{1}{3}\ln\frac{m_t^2}{Q^2} + \frac{N_f}{6}\ln\frac{m_{\tilde{q}}^2}{Q^2} + \frac{N_C}{3}\ln\frac{m_{\tilde{g}}^2}{Q^2}\right)\right]^{-1} \tag{9}$$

with the number of flavors $N_f = 6$ and colors $N_C = 3$. This procedure guarantees that the coupling $\alpha_s(Q^2)$ smoothly approaches the asymptotic form when $Q^2 \gg M^2$ for all masses M of the supersymmetric theory. In the calculations presented here we identify the renormalization scale with the c.m. energy.

After this introductory discussion of the individual channels and their dependence on the SUSY-QCD Yukawa coupling, detailed evaluations are presented in the following subsections.

2.1. Final-state supersymmetric particles

2.1.1. Squark pairs $\tilde{q}\tilde{q}$

It has been shown in Figs. 2 that the cross section for squark-pair production

$$e^+e^- \to \tilde{q}\tilde{q}^* \tag{10}$$

is maximal in the group of channels suited for the measurement of the SUSY-QCD Yukawa coupling. The cross section, in Born approximation,

$$\sigma_{LO}(e^+e^- \to \tilde{q}_{L/R}\,\tilde{q}^*_{L/R}) = \frac{\pi\alpha^2}{s} C_{L/R}\,\beta^3, \tag{11}$$

rises as the third power of the $\tilde{q}$ velocity $\beta = (1 - 4m_{\tilde{q}}^2/s)^{1/2}$ above the threshold as demanded for P-wave production [12]. The L/R couplings,

$$C_{L/R} = Q_q^2 + ({c_V^e}^2 + {c_A^e}^2)(c_V^q \pm c_A^q)^2\chi_Z^2 - 2Q_q c_V^e (c_V^q \pm c_A^q)\chi_Z \tag{12}$$

are given by the electric and isospin charges of the squarks, $c_V^f = (I_3^f - 2Q_f s_W^2)/s_{2W}$ and $c_A^f = I_3^f/s_{2W}$, where $s_W^2 = \sin^2\theta_W$ is the electroweak mixing parameter, $s_{2W} = \sin 2\theta_W$, and $\chi_Z = s/(s - m_Z^2)$ the scaled Z-propagator.

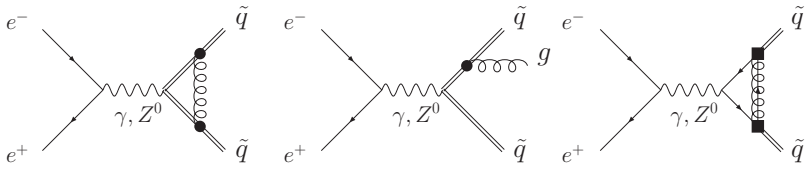

Figure 3: *Examples for diagrams of SUSY-QCD corrections to the production of squark pairs as defined in (13); left: gluon vertex correction, mid: gluon bremsstrahlung; right: gluino vertex correction.*

The production cross section for squark pairs in next-to-leading order (NLO) includes the gluon vertex correction and gluon bremsstrahlung, as well as the gluino vertex correction, as depicted in Fig. 3. [Final states $q\tilde{q}\tilde{g}$ are assumed to be separated explicitly.] The size of these corrections,

$$\sigma_{\rm NLO}(e^+e^- \to \tilde{q}\tilde{q}^* + \tilde{q}\tilde{q}^* g) = \sigma(e^+e^- \to \tilde{q}\tilde{q}^*)\big|_{\rm Born} \left[1 + \frac{4}{3}\frac{\alpha_s}{\pi}\Delta^{\rm vert+real}_{\rm gluon} + \frac{4}{3}\frac{\hat{\alpha}_s}{\pi}\Delta^{\rm vert}_{\rm gluino}\right], \tag{13}$$

depends on the masses of the squarks and gluinos, *cf.* Ref. [18]. The two parts contributing to the corrections are displayed, for the set of SPS1a parameters defined earlier, in Fig. 4. The gluon vertex contribution is formally divergent at the threshold, *i.e.* linearly in the inverse velocity of the squarks, but this Coulomb singularity is regularized by the non-zero squark width [19]. [*In toto*, the Born threshold suppression $\sim \beta^3$ is reduced to $\sim \beta^2$.] Compared to the Born cross section, $\mathcal{O}(50\,\text{fb})$, the corrections, in particular the gluino corrections involving the Yukawa coupling, are of order femtobarn. With an integrated luminosity ~ 1 ab^{-1}, these corrections can clearly manifest themselves beyond statistical fluctuations.

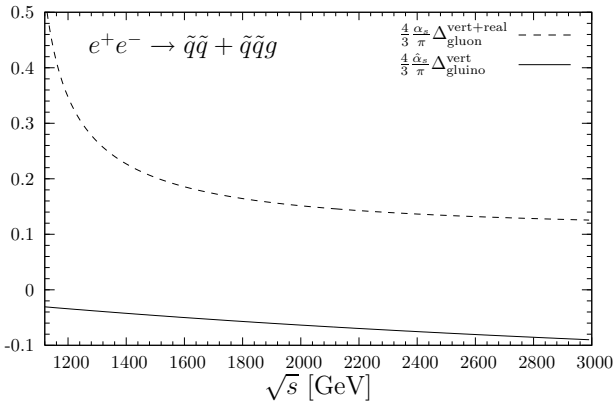

Figure 4: *The NLO SUSY-QCD (α_s and $\hat{\alpha}_s$) corrections for squark pair production. Separately shown are the sum of virtual and real gluon corrections, $(4\alpha_s/3\pi)\Delta^{vert+real}_{gluon}$, as well as the gluino vertex correction, $(4\hat{\alpha}_s/3\pi)\Delta^{vert}_{gluino}$. Parameters correspond to the reference point SPS1a.*

2.1.2. Squark-pair plus gluon final state $\tilde{q}\tilde{q}g$

A subset of final states in 2.1.1 is generated by the process

$$e^+e^- \to \tilde{q}\tilde{q}^* g \tag{14}$$

in which the gluon jet is isolated explicitly. This process measures the QCD coupling of gluons to squarks. The differential cross section in the scaled Dalitz variables $x_{\tilde{q}} = 2E_{\tilde{q}}/\sqrt{s}$, etc, was calculated already some time ago [20]:

$$\frac{d\sigma(e^+e^- \to \tilde{q}_{L/R}\,\tilde{q}^*_{L/R}\,g)}{dx_{\tilde{q}}\,dx_{\tilde{q}^*}} = \frac{\alpha^2\alpha_s}{4s}C_{L/R}\left[16 - \frac{16}{3}\frac{\mu^2_{\tilde{q}}y^2_{\tilde{q}}}{(1-x_{\tilde{q}})^2} - \frac{16}{3}\frac{\mu^2_{\tilde{q}^*}y^2_{\tilde{q}^*}}{(1-x_{\tilde{q}^*})^2} - \frac{8}{3}\frac{(2\mu^2_{\tilde{q}}-1)(y^2_{\tilde{q}}+y^2_{\tilde{q}^*}-y^2_g)}{(1-x_{\tilde{q}})(1-x_{\tilde{q}^*})}\right]. \tag{15}$$

To simplify the notation, the abbreviations $y_{\tilde{q}} = 2|\mathbf{p}_{\tilde{q}}|/\sqrt{s}$, $\mu_{\tilde{q}} = m_{\tilde{q}}/\sqrt{s}$, etc, have been introduced. If the squarks are lighter than the gluinos, as realized in SPS1a, the final state consists of three well-separated jets and a pair of neutralinos/charginos.

In the numerical example, Fig. 6, we assume a minimal energy to be carried by the jet(s) emitted in addition to the squark pair. The minimal energy $E_X > 100$ GeV required for X in the final state $\tilde{q}\tilde{q}X$ cuts out the infrared divergence in the gluon energy for $X = g$ in Born approximation. The dashed line in Fig. 6 corresponds to the Born approximation. The solid line adds the complete set of SUSY-QCD radiative corrections. These corrections include vertex and box diagrams as well as additional gluon-pair and light quark-antiquark final states. For these final states, $X = gg$ and $q\bar{q}$, the same cut-off in the energy ($E_X > 100$ GeV) is applied as before. Example diagrams for the radiative corrections are shown in Fig. 5. The semi-inclusive definition integrates out both the infrared and collinear singularities in the NLO corrected cross section.

In Born approximation the cross section depends strongly on the renormalization scale introduced solely by the

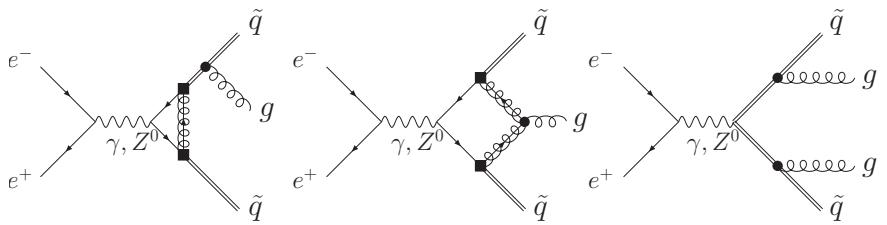

Figure 5: *Example diagrams for SUSY-QCD corrections to squark pair plus gluon production, left: gluino vertex correction, mid: box diagram; right: double gluon bremsstrahlung.*

gauge coupling. The dependence is significantly reduced if the higher order corrections are included. For example, varying the renormalization scale μ between $\frac{1}{5}\sqrt{s} \le \mu \le 5\sqrt{s}$ around a c.m. energy of $\sqrt{s} = 3$ TeV, the cross section varies by $\Delta\sigma/\sigma \simeq 14\%$ in Born approximation, while the variation is damped to 4% in NLO approximation.

In the peak region we find a sizeable cross section of several femtobarn. The radiative corrections enhance the cross section at a level of 20%.

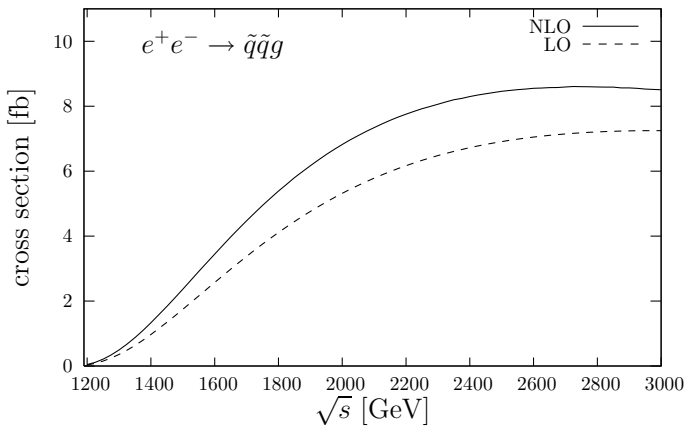

Figure 6: *Total cross section of the process $e^+e^- \to \tilde{q}\tilde{q}g$ for the c.m. energy $\sqrt{s}$ at leading order [dashed line] and next-to-leading order [full line]. The mass parameters are adopted from SPS1a. A minimal energy $E_X > 100$ GeV is assumed for single jets g and jet pairs gg, $\bar{q}q$ emitted off the squarks.*

2.2. The golden channel: Squark-gluino final states $q\tilde{q}\tilde{g}$

The golden channel for measuring the SUSY-QCD $q\tilde{q}\tilde{g}$ Yukawa coupling $\hat{g}_s$ *directly* is the process

$$e^+e^- \to q\tilde{q}^*\tilde{g} + c.c. \tag{16}$$

As evident from Fig. 1, the size of the cross section is governed by the quadratic dependence on the Yukawa coupling $\hat{g}^2 = 4\pi\hat{\alpha}_s$:

$$\begin{aligned}\frac{d^2\sigma}{dx_q\, dx_{\tilde{q}^*}} =& \frac{2\alpha^2\hat{\alpha}_s}{3s} C_{L/R}\Bigg\{ \frac{1}{(1-x_{\tilde{q}^*})^2} y^2_{\tilde{q}^*}(1 - x_{\tilde{q}^*} - \mu^2_{\tilde{g}} + \mu^2_{\tilde{q}^*}) \\ &+ \frac{1}{(1-x_q)^2}\left[3(1-x_q)(1-x_{\tilde{g}}) + 3\mu^2_{\tilde{g}} - 3\mu^2_{\tilde{q}^*} - x_q^2(\mu^2_{\tilde{g}} - \mu^2_{\tilde{q}^*}) - \frac{1}{2}(1-x_q)(y_q^2 - y^2_{\tilde{g}} + y^2_{\tilde{q}^*})\right] \\ &+ \frac{1}{(1-x_q)(1-x_{\tilde{q}^*})}\left[x_q y^2_{\tilde{q}^*} - \frac{1}{2}(x_{\tilde{q}^*} + 2\mu^2_{\tilde{g}} - 2\mu^2_{\tilde{q}^*})(y_q^2 - y^2_{\tilde{g}} + y^2_{\tilde{q}^*})\right]\Bigg\},\end{aligned} \tag{17}$$

in the standard notation introduced before.

The Born cross sections for both the cases $m_{\tilde{q}} < m_{\tilde{g}}$ and $m_{\tilde{q}} > m_{\tilde{g}}$ are presented in Figs. 2. The processes give rise to 4, respectively 6 jets in the final state [at Born level], with the 4-jet final state characteristic for $q\tilde{q}\tilde{g}$ production in the mass range $m_{\tilde{q}} < m_{\tilde{g}}$.

Examples of NLO diagrams contributing to the SUSY-QCD corrections to $q\tilde{q}\tilde{g}$ final states are depicted in Fig. 7.

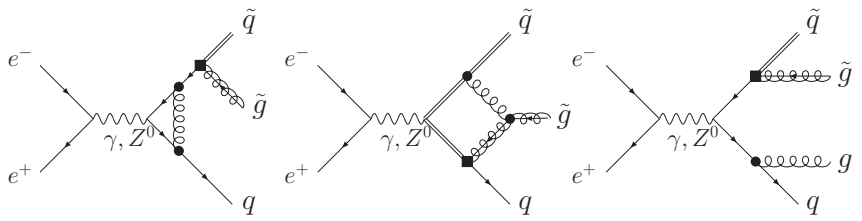

Figure 7: *Example diagrams for SUSY-QCD corrections to squark gluino production, left: gluon vertex correction, mid: box diagram; right: real gluino emission.*

Vertex and box diagrams are built up by gluinos, gluons, squarks and quarks. To order α_s, 4-parton final states are generated only by the emission of an additional gluon. Since the radiatively corrected cross section is defined inclusively, infrared and collinear singularities are integrated out.

The corrected cross sections are displayed in Figs. 8 for squarks lighter and heavier than gluinos [SPS1a and SPS1a reversed], respectively. Again, the strong dependence on the renormalization scale in Born approximation is damped once the higher order corrections are included properly: If the renormalization scale μ varies between $\frac{1}{5}\sqrt{s} \le \mu \le 5\sqrt{s}$, for $\sqrt{s} = 3$ TeV the cross section for $m_{\tilde{q}} < m_{\tilde{g}}$ varies by $\Delta\sigma/\sigma \simeq 14\%$ in Born approximation, while the variation is damped to 4% in NLO approximation.

The cross sections for $m_{\tilde{q}} < m_{\tilde{g}}$ are enhanced by the radiative corrections to a size of order 2 fb which can be considered sufficient for experimental analysis if integrated luminosities ~ 1 ab^{-1} can be achieved. In the mass range $m_{\tilde{q}} > m_{\tilde{g}}$ the size of the cross section is rather small, however.

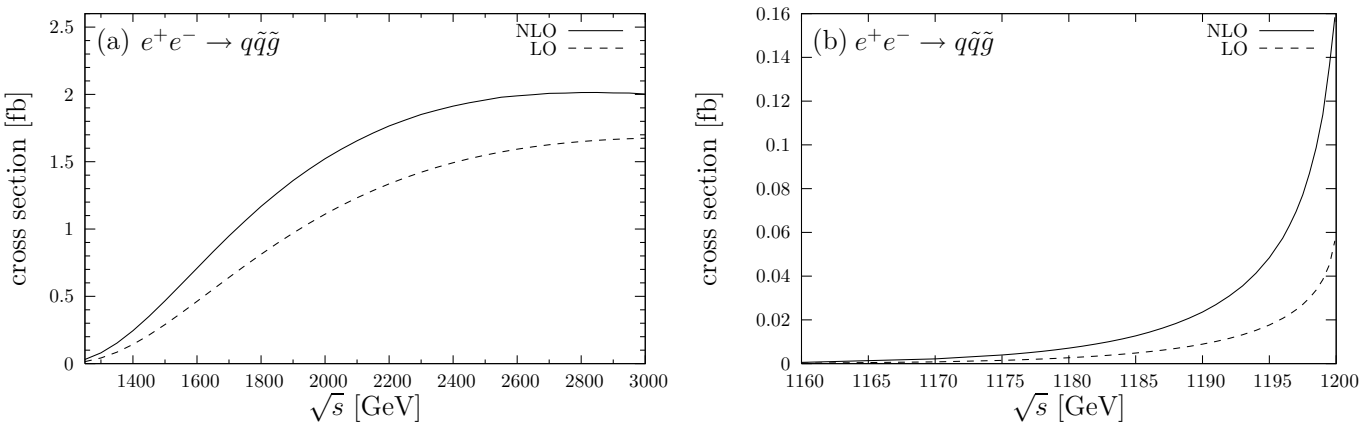

Figure 8: *(a) Total cross section for squark-gluino production at LO and NLO for SPS1a mass parameters, i.e. $m_{\tilde{q}} < m_{\tilde{g}}$; (b) for reversed SPS1a mass parameters, i.e. $m_{\tilde{q}} > m_{\tilde{g}}$. [Above a c.m. energy of twice the squark mass, squark-pair production followed by squark decays to quarks and gluinos, is by far dominant.]*

2.3. Final states without supersymmetric particles

2.3.1. Quark pairs qq

The basic quark-pair production process, defined in the absence of any supersymmetric particle in the final state,

$$e^+e^- \to q\bar{q} \tag{18}$$

scales asymptotically with the energy squared:

$$\sigma(e^+e^- \to q\bar{q})\big|_{\text{Born}} = \frac{4\pi\alpha^2}{s}\left[Q_q^2 + ({c_V^e}^2 + {c_A^e}^2)({c_V^q}^2 + {c_A^q}^2)\chi_Z^2 - 2Q_q c_V^e c_V^q \chi_Z\right] . \tag{19}$$

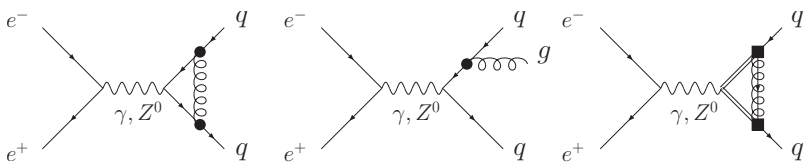

Figure 9: *Examples for diagrams of QCD and SUSY-QCD corrections to the production of quark pairs; left: gluon vertex correction, mid: gluon bremsstrahlung; right: squark/gluino vertex correction.*

The Born cross section is modified, to NLO, by gluon exchanges in the vertex and by gluon bremsstrahlung, as well as squark/gluino corrections to the vertex, Fig. 9,

$$\sigma_{\text{NLO}}(e^+e^- \to q\bar{q}) = \sigma(e^+e^- \to q\bar{q})\big|_{\text{Born}}\left(1 + \frac{4}{3}\frac{\alpha_s}{\pi}\Delta_{\text{gluon}}^{\text{vert+real}} + \frac{4}{3}\frac{\hat{\alpha}_s}{\pi}\Delta_{\text{squ/gluino}}^{\text{vert}}\right) . \tag{20}$$

The gluon correction to NLO is well known, $\Delta_{\text{gluon}}^{\text{vert+real}} = 3/4$, while the genuine triangular squark/gluino correction is more involved [21]. For the set of SPS1a and reversed SPS1a mass parameters introduced before, the pure QCD corrections are in general leading, except for very high energies. The individual gluon and SUSY corrections are presented in Fig. 10. [The two contributions are separately gauge invariant.] The Born cross section drops from 2.2 pb down to 61 fb in the range of c.m. energies between 0.5 and 3 TeV. The genuine SUSY-QCD corrections involving the Yukawa coupling of squarks to quarks and gluinos are moderately large and of half the size of the standard QCD corrections. In the peak region the radiative SUSY corrections are of the order of 1.5%; the corrections flip sign at

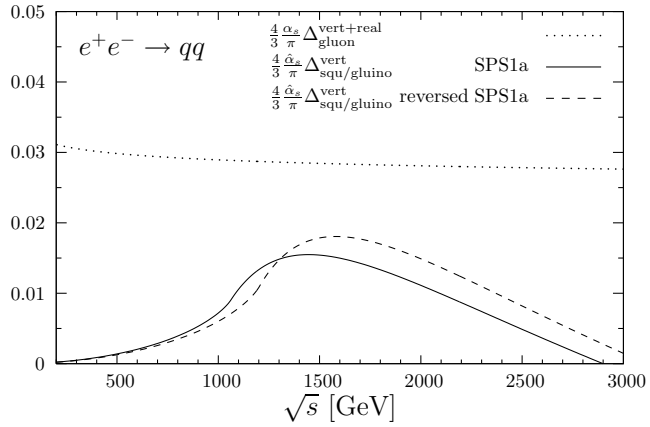

Figure 10: *NLO QCD, $(4\alpha_s/3\pi)\Delta^{vert+real}_{gluon}$, as well as NLO SUSY-QCD, $(4\hat\alpha_s/3\pi)\Delta^{vert}_{squ/gluino}$, corrections of the total cross section for quark pair production in the reference points SPS1a and reversed SPS1a.*

an energy of ~ 3 TeV for the two reference sets of SUSY masses. For $m_{\tilde q} = m_{\tilde g} \equiv \tilde M$ the correction can be cast in the compact form

$$\Delta^{\rm vert}_{\rm squ/gluino} = \frac{3}{4} + \frac{\beta}{4}\ln\left(\frac{1-\beta}{1+\beta}\right) + \frac{1}{16}(1-\beta^2)\left[\ln^2\left(\frac{1-\beta}{1+\beta}\right) - \pi^2\right], \tag{21}$$

where $\beta = (1-4\tilde M^2/s)^{1/2}$. The SUSY correction approaches

$$\Delta^{\rm vert}_{\rm squ/gluino} = -1/4\ \ln(s/\tilde M^2) \tag{22}$$

for asymptotic energies. The logarithmic behavior in the energy is consistent with the Lee-Nauenberg theorem since gluino radiation is not included in the final state; in fact, adding gluino radiation cancels the logarithm in the asymptotic region.

2.3.2. Quark Pairs and Gluons qqg

If additional gluon jets are isolated in the final state,

$$e^+e^- \to q\bar q g\,, \tag{23}$$

the analysis becomes much more complex. Starting from the Dalitz plot density for gluon radiation [22],

$$\left.\frac{d^2\sigma(e^+e^- \to q\bar q g)}{dx_q dx_{\bar q}}\right|_{\rm Born} = \sigma(e^+e^- \to q\bar q)\big|_{\rm Born}\ \frac{2\alpha_s}{3\pi}\frac{x_q^2 + x_{\bar q}^2}{(1-x_q)(1-x_{\bar q})}\,, \tag{24}$$

with the scaled energies $x_q = 2E_q/\sqrt{s}$ etc, the jet events are defined for a cut in the invariant masses of the parton pairs $y_{ij} = (p_i+p_j)^2/s > 0.05$. The radiative corrections may be decomposed in the form

$$\sigma_{\rm NLO}(e^+e^- \to q\bar q g) = \sigma(e^+e^- \to \bar q q g)\big|_{\rm Born}\left(1 + \frac{\alpha_s}{\pi}\Delta^{\rm vert+real}_{\rm gluon} + \frac{\hat\alpha_s}{\pi}\Delta^{\rm vert}_{\rm squ/gluino}\right). \tag{25}$$

As generally anticipated for corrections to jet cross-sections, the gluon corrections, *c.f.* Ref. [23],

$$\frac{\alpha_s}{\pi}\Delta^{\rm vert+real}_{\rm gluon} \simeq \frac{\alpha_s}{\pi}\frac{B}{2A} \tag{26}$$

are by far dominant with $B/2A \simeq 10$ for $y_{ij} = 0.05$, *i.e.* $\frac{\alpha_s}{\pi}\Delta^{\rm vert+real}_{\rm gluon} \simeq 0.3$. The genuine SUSY-QCD corrections are defined as any corrections involving propagators of supersymmetric particles, some examples are shown in Fig. 11. Such diagrams come with two powers of the quark-squark-gluino Yukawa coupling at next-to-leading order. The genuine SUSY contribution $\frac{\hat\alpha_s}{\pi}\Delta^{\rm vert}_{\rm squ/gluino}$ is displayed in Fig. 12. The two mass hierarchies $m_{\tilde q} < m_{\tilde g}$ and $m_{\tilde q} > m_{\tilde g}$ are adopted again from the reference point SPS1a and the reversed SPS1a point. In the respective peak regions SUSY corrections of about 1.5% are predicted, significantly smaller than the standard QCD corrections, as anticipated.

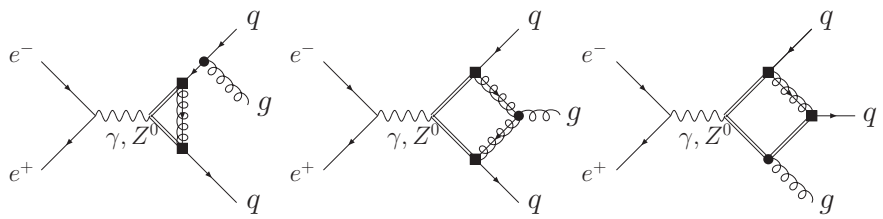

Figure 11: *Examples for diagrams of SUSY-QCD corrections to the production of quark pairs accompanied by a gluon; left: squark/gluino vertex correction, mid and right: squark/gluino box correction.*

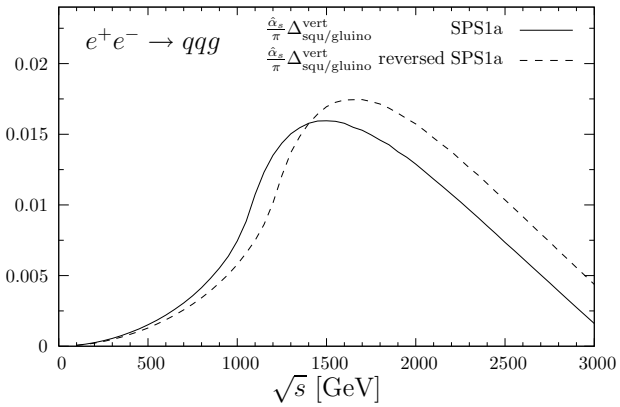

Figure 12: *NLO SUSY-QCD corrections, $(\hat{\alpha}_s/\pi)\Delta^{vert}_{squ/gluino}$, to the total cross section for $q\bar{q}g$ production for the mass hierarchies of SPS1a, solid line, and SPS1a reversed, dashed line.*

3. Assessment

In the preceding section the theoretical base has been studied for future measurements of the Yukawa coupling between quarks, squarks and gluinos in high-energy e^+e^- collisions. Supersymmetry predicts this coupling to be identical with the standard QCD gauge coupling between quarks and gluons, and squarks and gluons. Various channels have been investigated which can be explored to test this fundamental identity between the couplings, either indirectly through virtual corrections to quark and squark pair production in e^+e^- collisions, or directly in comparing the cross section for the golden channel $q\tilde{q}\tilde{g}$ with the standard gluon radiation processes qqg and $\tilde{q}\tilde{q}g$. While the golden channel measures the $q\tilde{q}\tilde{g}$ Yukawa coupling $\hat{g}_s$, the radiation processes $\tilde{q}\tilde{q}g$ and qqg determine the QCD gauge coupling g_s in the squark sector and the standard quark sector for comparison.

The central results are summarized in Tab. II and Figs. 13. In the table the SUSY parameters are adopted from the reference point SPS1a with squark and gluino masses of 530 GeV and 600 GeV, respectively. Since by the time of measurements of the couplings the squark and gluino masses will be determined accurately, special values of the e^+e^- c.m. energy can be chosen such as to maximize the sensitivity for the measurements of the Yukawa and gauge couplings. A standard value $\int \mathcal{L} = 1$ ab^{-1} is taken for the integrated luminosity. The errors quoted in the table are purely *statistical*, reflecting the minimal errors that can be expected in any future experimental analysis.

The left-most figure in the panel Figs. 13 displays the contours of the *statistical* 1-sigma errors $\Delta\hat{\alpha}_s/\hat{\alpha}_s$ for the standard qq channel in the $[m_{\tilde{q}}, m_{\tilde{g}}]$ mass plane for ILC, irrespective of any specific model except SUSY-QCD. For each $\tilde{q}, \tilde{g}$ mass pair the collider energy is chosen such as to provide maximal sensitivity to the measurement of $\hat{\alpha}_s$. The Yukawa coupling $\hat{\alpha}_s$ can be determined in this channel only indirectly through virtual SUSY corrections. Such analyses may provide a first glimpse of the Yukawa coupling.

	Born coupling	$\sqrt{s}\{\max\}$[GeV]	$\sigma_{\rm Born}$ [fb]	$\sigma_{\rm NLO}$ [fb]	$\frac{4}{3}\frac{\alpha_s}{\pi}\Delta_{\rm QCD}$	$\frac{4}{3}\frac{\hat\alpha_s}{\pi}\Delta_{\rm SUSY}$	$\Delta\hat\alpha_s/\hat\alpha_s$
$\tilde q\tilde q$		3,000	25.1	26.0	0.126	−0.09	7.0%
qq		1,300	328	342	0.0277	0.0159	11%
$q\tilde q\tilde g$	$\hat\alpha_s$	2,850	1.66	2.01	0.661	−0.448	2.5%
					$\frac{\alpha_s}{\pi}\Delta_{\rm QCD}$	$\frac{\hat\alpha_s}{\pi}\Delta_{\rm SUSY}$	$\Delta\alpha_s/\alpha_s$
$\tilde q\tilde q g$	α_s	2,800	7.21	8.59	0.276	−0.0836	1.2%
qqg	α_s	2,800	10.5	13.1	0.257	0.0039	1.0%

Table II: *1-sigma statistical errors of the Yukawa $\hat\alpha_s$ and gauge α_s couplings determined from quark-squark-gluino final states and SUSY radiative corrections in various channels based on SPS1a SUSY parameters. The upper part of the table with the final states $\tilde q\tilde q$, qq and $q\tilde q\tilde g$ describes the measurement of $\hat\alpha_s$, and the lower part, with $\tilde q\tilde q g$ and qqg, the measurement of α_s. The c.m. energy $\sqrt{s}\{max\}$ is chosen, below 3 TeV, such that the sensitivity to the measurement of the couplings is maximized, except for the gauge coupling in qqg where the scale is adjusted to $\tilde q\tilde q g$.*

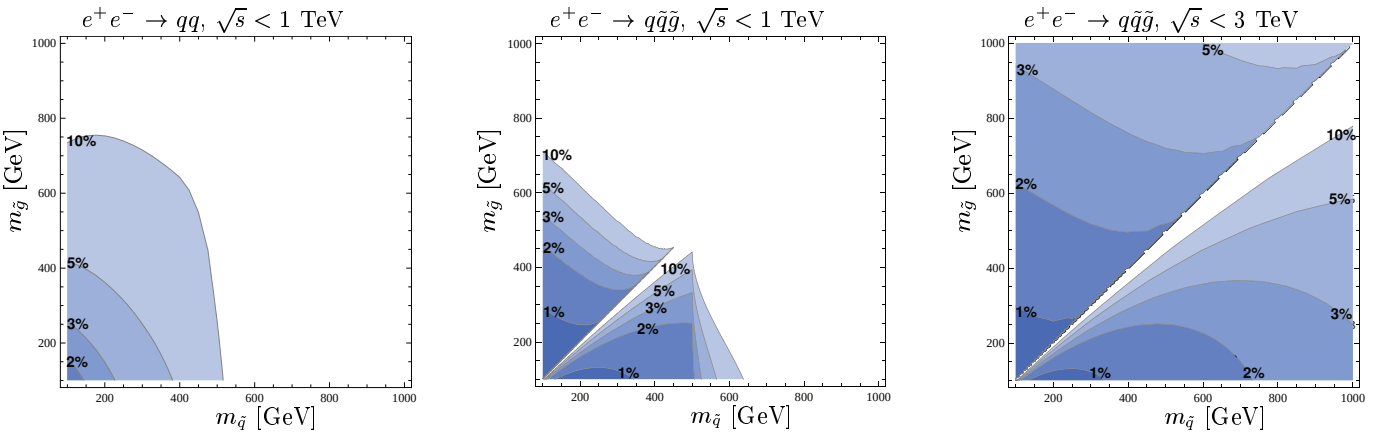

Figure 13: *Contours of the statistical 1-sigma errors of the Yukawa coupling $\Delta\hat\alpha_s/\hat\alpha_s$ in the $[m_{\tilde q}, m_{\tilde g}]$ mass plane,* Left*: for the indirect channel $e^+e^- \to qq$ at ILC energies;* Mid, Right*: for the direct golden channel $e^+e^- \to q\tilde q\tilde g$, corresponding to a maximal ILC c.m. energy of* 1 TeV*, and to* 3 TeV *for CLIC, respectively. The blind wedge can be covered by analyzing the partial widths.*

The figures in the middle and on the right of the panel summarize *statistical* analyses of the golden $q\tilde q\tilde g$ channel on the same basis. In this channel the Yukawa coupling can be measured directly since the Born cross section is proportional to $\hat\alpha_s$. The results are presented for ILC c.m. energies up to a maximum of 1 TeV, and for CLIC up to 3 TeV. As before, the energies are chosen at the point of maximal sensitivity for the Yukawa coupling for any mass pair $[m_{\tilde q}, m_{\tilde g}]$. For $m_{\tilde g} < m_{\tilde q}$ the collider energy is restricted to the range below the $\tilde q\tilde q$ threshold as to avoid contamination of the $q\tilde q\tilde g$ channel due to on-shell $\tilde q \to q\tilde g$ decays. This restriction generates a blind wedge near the threshold which however can be covered in analyses of the partial widths as discussed before.

The estimate of the statistical error $\Delta\hat g_s/\hat g_s \simeq 1\%$ for the measurement of the Yukawa coupling in this report is only a first step. The step is promising, nevertheless, as the expected error is sufficiently small. Even if an order of magnitude of events is lost due to experimental cuts and efficiencies in controlling, for example, the chargino and neutralino modes of squark decays [and cascading gluinos], the resulting final error is still at a level of 5 to 10%. This size compares reasonably well with expectations for LHC experimental analyses in Ref. [4] in which squark/gluino decays are included explicitly. Thus, LHC and a TeV lepton collider are complementary instruments for the involved measurements of the SUSY-QCD Yukawa and gauge couplings. In particular, since the relevant cross sections drop

with rising squark and gluino masses quadratically and faster[2], mutual complementarity of the two methods raises prospects of testing the identity of Yukawa and gauge couplings in super-QCD considerably.

Acknowledgments

Thanks go to M. Spira, S. Dittmaier and D. Zerwas for helpful discussions. PMZ is grateful to the Inst. Theor. Phys. E for the warm hospitality extended to him at RWTH Aachen. The work of AB was supported by a Heisenberg grant of the DFG. The work of MW was supported in part by the National Science Foundation under grant NSF-PHY-0547564.

References

[1] P. Fayet, Phys. Lett. B **69**, 489 (1977).
[2] S. Dimopoulos and H. Georgi, Nucl. Phys. B **193**, 150 (1981).
[3] N. Sakai, Z. Phys. C **11**, 153 (1981).
[4] A. Freitas and P. Z. Skands, JHEP **0609** (2006) 043 [hep-ph/0606121]; A. Freitas, P. Z. Skands, M. Spira and P. M. Zerwas, JHEP **0707** (2007) 025, [hep-ph/0703160].
[5] J. A. Aguilar-Saavedra *et al.* [ECFA/DESY LC Physics Working Group], *Physics at an e^+e^- Linear Collider*, [hep-ph/0106315]; A. Djouadi, *et al.*, *Physics at the ILC*, [0709.1893 hep-ph].
[6] E. Accomando *et al.* [CLIC Physics Working Group], *Physics at the CLIC multi-TeV linear collider*, [hep-ph/0412251].
[7] J. R. Ellis, S. Heinemeyer, K. A. Olive, A. M. Weber and G. Weiglein, JHEP **0708** (2007) 083 [0706.0652 hep-ph].
[8] S. Y. Choi, J. Kalinowski, G. A. Moortgat-Pick and P. M. Zerwas, Eur. Phys. J. C **22** (2001) 563 [Addendum-ibid. C **23** (2002) 769], [hep-ph/0108117] and [hep-ph/0202039]; A. Freitas, A. von Manteuffel and P. M. Zerwas, Eur. Phys. J. C **34** (2004) 487, [hep-ph/0310182].
[9] S. Berge and M. Klasen, Phys. Rev. D **66** (2002) 115014, [hep-ph/0208212].
[10] A. Brandenburg, M. Maniatis and M. M. Weber, *SUSY02, Hamburg 2002*, [hep-ph/0207278].
[11] G. Weiglein *et al.* [LHC/LC Study Group], Phys. Rept. **426** (2006) 47 [hep-ph/0410364].
[12] S. Y. Choi, K. Hagiwara, H. U. Martyn, K. Mawatari and P. M. Zerwas, Eur. Phys. J. C **51** (2007) 753 [hep-ph/0612301].
[13] B. C. Allanach *et al.*, in *Proceedings, APS/DPF/DPB Summer Study on the Future of Particle Physics, Snowmass 2001*, and Eur. Phys. J. C **25** (2002) 113, [hep-ph/0202233].
[14] T. Affolder *et al.* [CDF Collaboration], Phys. Rev. Lett. **88** (2002) 041801, [hep-ex/0106001].
[15] W. Beenakker, R. Hopker and P. M. Zerwas, Phys. Lett. B **378** (1996) 159, [hep-ph/9602378].
[16] W. Hollik and D. Stockinger, Eur. Phys. J. C **20**, 105 (2001), [hep-ph/0103009]; S. P. Martin and M. T. Vaughn, Phys. Lett. B **318** (1993) 331 [hep-ph/9308222].
[17] S. Bethke, Prog. Part. Nucl. Phys. **58** (2007) 351 [hep-ex/0606035].
[18] A. Arhrib, M. Capdequi-Peyranere and A. Djouadi, Phys. Rev. D **52** (1995) 1404 [hep-ph/9412382].
[19] A. Freitas, D. J. Miller and P. M. Zerwas, Eur. Phys. J. C **21** (2001) 361 [hep-ph/0106198]; V. S. Fadin and V. A. Khoze, *Proceedings, 24th LNPI Winter School, Leningrad 1989.*
[20] H. D. Dahmen, D. H. Schiller and D. Wahner, Nucl. Phys. B **227** (1983) 291.

[2]Since analytical expressions for cross sections at next-to-leading order are quite involved, they are not noted here explicitly, but they can be retrieved from http://www.thphys.uni-heidelberg.de/∼maniatis/susyqcd.

[21] K. Hagiwara and H. Murayama, Phys. Lett. B **246**, 533 (1990); A. Djouadi, M. Drees and H. Konig, Phys. Rev. D **48**, 3081 (1993) [hep-ph/9305310]; A. Brandenburg and M. Maniatis, Phys. Lett. B **558**, 79 (2003) [hep-ph/0301142].

[22] J. R. Ellis, M. K. Gaillard and G. G. Ross, Nucl. Phys. B **111** (1976) 253 [Erratum-ibid. B **130** (1977) 516]; P. Hoyer, P. Osland, H. G. Sander, T. F. Walsh and P. M. Zerwas, Nucl. Phys. B **161** (1979) 349.

[23] S. Bethke, Z. Kunszt, D. E. Soper and W. J. Stirling, Nucl. Phys. B **370** (1992) 310 [Erratum-ibid. B **523** (1998) 681].